MONTE CARLO SIMULATIONS OF MUON PRODUCTION

Robert B. Palmer, Juan C. Gallardo, Richard C. Fernow, Yağmur Torun
Brookhaven National Laboratory
P. O. Box 5000, Upton, New York 11973-5000

David Neuffer
CEBAF
Newport News, VA, 23606

David Winn
Fairfield University,
Fairfield, CT, 06430-5195

Abstract

Muon production requirements for a muon collider are presented. Production of muons from pion decay is studied. Lithium lenses and solenoids are considered for focussing pions from a target, and for matching the pions into a decay channel. Pion decay channels of alternating quadrupoles and long solenoids are compared. Monte Carlo simulations are presented for production of $\pi \rightarrow \mu$ by protons over a wide energy range, and criteria for choosing the best proton energy are discussed.

1 INTRODUCTION

The luminosity $\mathcal{L}$ of a muon collider is given by

$$\mathcal{L} = \frac{N^2 \gamma n_t f}{4\pi\beta^* \epsilon_n} \tag{1}$$

where N is the number of muons per bunch, γ is the energy per beam divided by the muon mass, n_t is the effective number of turns made by the muons before they decay, f is the repetition frequency, β^* is the Courant-Snyder parameter at the focus, and ϵ_n is the r.m.s. normalized emittance of the beams (assumed symmetric in x and y). In order to obtain a reasonable event rate, the luminosity must be proportional to the center of mass energy squared and may be taken to be of the order of $\mathcal{L} \geq 10^{33}\ E_{cm}^2\ cm^{-2}s^{-1}$ where E_{cm} is the energy in TeV. Possible parameters that would yield a luminosity close to this requirement, at 4 TeV in the center of mass, are given in Table 1.

Beam energy	TeV	2
Beam γ		19,000
Repetition rate f	Hz	30
Muons per bunch N	10^{12}	2
Bunches of each sign		1
Normalized rms emittance ϵ_n	mm mrad	50
Average ring mag. field	Tesla	6
Effective turns before decay n_t		900
β^* at intersection	mm	3
Luminosity $\mathcal{L}$	$cm^{-2}s^{-1}$	10^{35}

Table 1: Parameters of a 4 TeV center of mass $\mu^+\mu^-$ Collider

The value of the emittance ϵ_n used is limited by the technology used to cool the beams, and is chosen here to be consistent with that believed (1) obtainable with ionization cooling. The intersection point (IP) β^* will be limited by the design of the chromatic correction system at the IP, and by the achievable bunch length. The value given here is believed to be technically possible. The number of turns n_t is set by the average bending field in the collider ring. The value taken here corresponds to a mean field of 6 Tesla, which is probably as high as is technically feasible. The repetition rate f is taken to be 30 Hz, and is constrained by proton source, power consumption, and radiation considerations.

With the above parameters, the required luminosity is achieved, but the number of muons per bunch N is large ($2\ 10^{12}$). Stacking many smaller muon bunches to achieve such a population would be hard because of the life time limitations of the muons. Thus if the proton bunch population is to be kept reasonable, the production must be efficient, i.e. we require a high value of the number of captured muons per initial proton $\eta_\mu = n_\mu/n_p$.

Since pion multiplicity rises with proton energy, the value of η_μ tends also to rise with the proton energy used. But if the energy is allowed to rise, then the cost and energy consumption of the proton source will also rise. Thus the requirement is for the highest number of muons per proton η_μ, at the lowest possible proton energy E_p.

2 THEORY

2.1 Introduction

We consider muons made by the decay of pions generated by the interaction of a proton beam with a metal target. With 30 GeV protons, the pion multiplicity

is of the order of one. Almost every pion made, if it does not interact in the target or otherwise get lost, will decay into a muon. The potential value of η_μ is thus of the order of one. At proton energies lower than 30 GeV, the multiplicity falls, but remains substantial until below the N^* resonance (at $E_p = 0.73\,GeV$). The challenge is to target efficiently and capture as large a fraction of the pions as possible; then to capture as large a fraction as possible of the muons from their decay.

Previous estimates (2) of the efficiency of such capture were low ($\approx 10^{-3}$), and only moderate luminosity was possible. Such estimates assumed conventional focussing technology and decay channels with restricted momentum acceptances ($\pm 5\%$). In this case, the values of η_μ are proportional to the square of the momentum acceptances; one factor from the fraction of pions accepted from the target, and another from the fraction of muons accepted from the decay of those pions. Since the luminosity per pulse is proportional to the square of the number of muons, the luminosity goes as the fourth power of the acceptances. If these acceptances can be raised, then a major improvement in η_μ may be expected.

In this paper we discuss two methods of capturing pions from the production target: a) lithium lenses followed by a decay channel consisting of alternating quadrupoles, and b) a high field solenoid matched adiabatically to a lower field solenoid decay channel.

2.2 Lithium Lenses and Quadrupole Channel

2.2.1 Capture from target

The Courant-Snyder parameter β in a long lithium lens, assuming uniform current density, is

$$\beta = \frac{p\,\theta_{max}}{B_{max}\,c} \tag{2}$$

where p is the particle momentum in eV/c, c is the velocity of light. If θ_{max} is the maximum angular amplitude accepted, and B_{max} is the field on the surface, its radius a is

$$a = \beta\,\theta_{max} = \frac{p\,\theta_{max}^2}{B_{max}\,c} \tag{3}$$

Inserting the target inside the lithium lens maximizes the yield of captured pions. The required length ℓ_1 of the lens is half the betatron wavelength, $\lambda/2$; if we express the maximum angle θ_{max} as $\hat{p}_t/p$ then,

$$\ell_1 = \frac{\pi}{2}\,\frac{\hat{p}_t}{B_{max}\,c}, \tag{4}$$

which, for a given transverse momentum acceptance, is independent of the momentum p. The radius a_1 of the lens is

$$a_1 = \frac{\hat{p}_t^2}{B_{max}\ c}\ \frac{1}{p} \tag{5}$$

which rises as the momentum falls. For $B_{max} = 10\ T$, and a nearly ideal $\hat{p}_t = 0.6\ GeV/c$, then $\ell_1 = 0.31\ m$. The radius will be 12 cm at 1 GeV/c, falling to 3 cm at 4 GeV/c.

The required current I is

$$I = \frac{2\pi\ \hat{p}_t^2}{\mu_o\ c\ p} \tag{6}$$

which falls as the momentum rises, independent of the surface field. For $\hat{p}_t = 0.6\ GeV/c$, the current falls from a value of 6 MA at 1 GeV/c to 1.5 MA at 4 GeV/c.

These currents and radii are far larger than those in currently used lenses (eg FNAL: a=1 cm, I=0.5 MA), but they may still be possible. The temperature rise and central pressures are proportional only to the surface field, and this we kept constant. However, it is clear that this type of focussing is better suited to the higher momenta.

At a fixed momentum, the normalized total emittance of the resulting beam $\epsilon_{tn}(tgt)$ is set by the target length ℓ_{tgt}

$$\epsilon_{tn}(tgt) = \frac{\ell_{tgt}}{2}\ \frac{\hat{p}_t^2}{m_\pi\ p} \tag{7}$$

where m_π is the pion mass in units of eV/c^2 and the momenta p and $\hat{p}_t$ are in units of eV/c. At 1 GeV/c, a target length of 0.18 m (for Cu), and a maximum $\hat{p}_t$ of 0.6 GeV/c, the emittance has a value of 0.23 m, but has fallen to a 0.06 m at 4 GeV/c.

For a point source, with momentum spread $\frac{dp}{p} = \delta$, the total normalized emittance $\epsilon_{tn}(mom)$ is

$$\epsilon_{tn}(mom) = \frac{\pi}{2}\ \frac{\hat{p}_t^3\ \delta}{B_{max}\ c\ m_\pi\ p} \tag{8}$$

which also falls with momentum. This equals the emittance for target length when

$$\delta = \frac{\ell_{tgt}\ B_{max}\ c}{\pi\ \hat{p}_t} \tag{9}$$

which for the above parameters is ± 0.28.

2.2.2 Quadrupole channel

The focussing strength k (defined to be the inverse of the focal length) of a thin quadrupole lens is

$$k = \frac{\ell_q \; B_{pole} \; c}{ap} \tag{10}$$

where B_{pole} is the pole field at the pole radius a, and the momentum p is in eV/c. If the phase advance per cell is ψ, and a half cell length is ℓ_h, then

$$s \; = \; \sin\frac{\psi}{2} \; = \; \frac{\ell_h \; k}{2} \tag{11}$$

The average β is $2\ell_h/\psi$ and the maximum β is

$$\beta_{max} \; = \; \frac{2}{k}\sqrt{\frac{1+s}{1-s}} \tag{12}$$

Thus, the unnormalized acceptance of a quadrupole channel varies inversely with the momentum

$$\mathcal{A} = \frac{a^2}{\beta_{max}} = \frac{a\ell_q B_{pole} c}{2p}\sqrt{\frac{1-s}{1+s}} \tag{13}$$

$\mathcal{A}$ is zero until the momentum has risen to the value p_{min} corresponding to the onset of the stop band at a phase advance per cell of π. This minimum accepted momentum is

$$p_{min} = \frac{\ell_q^2}{F}\frac{B_{pole} c}{2a}, \tag{14}$$

where $F = \ell_q/\ell_h$ is the fraction of length full of quads. For nominal capture of 1 GeV/c pions we require a p_{min} of the order of $p/4 = 0.25 \; GeV/c$. Then for $B_{pole} = 6 \; T$, $a = 0.15 \; m$ and $F = 1/2$, then we obtain $\ell_q = 0.14 \; m$. For higher momenta ℓ_q should be increased as the square root of the momentum.

The unnormalized acceptance rises to a maximum at a momentum of approximately 4 times this minimum, and then falls slowly. The normalized acceptance $\mathcal{A}_n = \gamma\beta\mathcal{A}$ rises continuously, approaching an asymptotic value of

$$\mathcal{A}_n(quad) = \frac{\ell_q a B_{pole} c}{2m_\pi} \tag{15}$$

Fig. 1 shows the normalized acceptances for lattices with quadrupole lengths ℓ_q of 14, 20 and 30 cm, corresponding to optimized designs for proton energies of 10, 30, and 100 GeV. A fixed value of $F = 1/2$ is assumed. It is seen that for longer quadrupoles, the maximum acceptance is increased, but the minimum momentum rises.

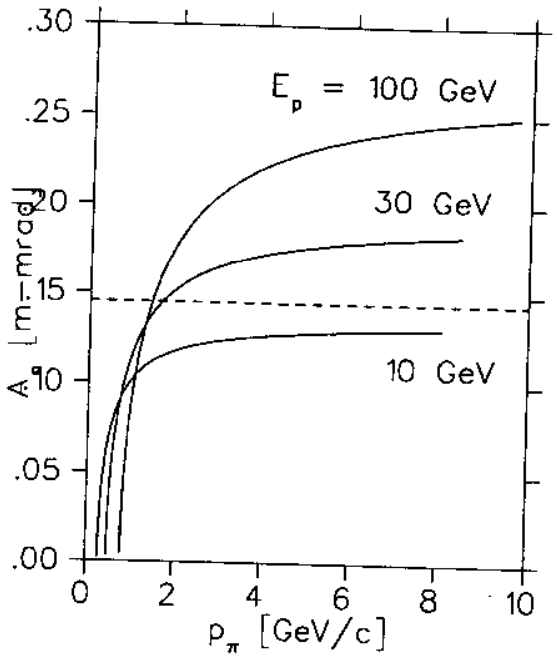

Figure 1: Decay Channel Acceptances. Continuous lines are for quadrupole channels optimized for proton energies E_p = 10, 30, and 100 GeV by adjusting the quadrupole lengths; dashed line is acceptance for a solenoid channel with the same field.

2.2.3 Matching

Matching from the first lens into the channel is challenging. The beam size after the lens is usually significantly smaller than the aperture of the channel. An adiabatically tapered lithium lens transition would be ideal, providing a match at all momenta, but would involve too much beam loss from interactions in the lithium. Instead we consider a two lens match that is similar in function to the multiple horns used in neutrino beams (3).

We consider first a single lens focus. The solid line in Fig. 2a shows the ratio of outgoing angles over incoming angles, for a single thin lens of focal length 20 cm, set to focus 2 GeV/c momentum particles. θ_{out}/θ_{in} is less than 1/3 over the momentum range of about 1.5 GeV/c. The dotted lines show the same ratios for particles starting at 9 cm in front or behind the nominal source, i.e. they represent particles coming from the ends of an 18 cm target.

Fig. 2b shows the same thing for a two thin lens system. The second lens has a focal length 3 times that of the first, and both are placed at distances from the source equal to their focal lengths. It is seen that there are now two momenta for which the outgoing angles are zero, and the range of momenta for which θ_{out}/θ_{in} is less than 1/3 is now 5 GeV/c, compared with only 1.5 GeV

for the single lens case. The effect of displacing the source is to smear the distributions, but leave a net reduction of angles over the same wide momentum range.

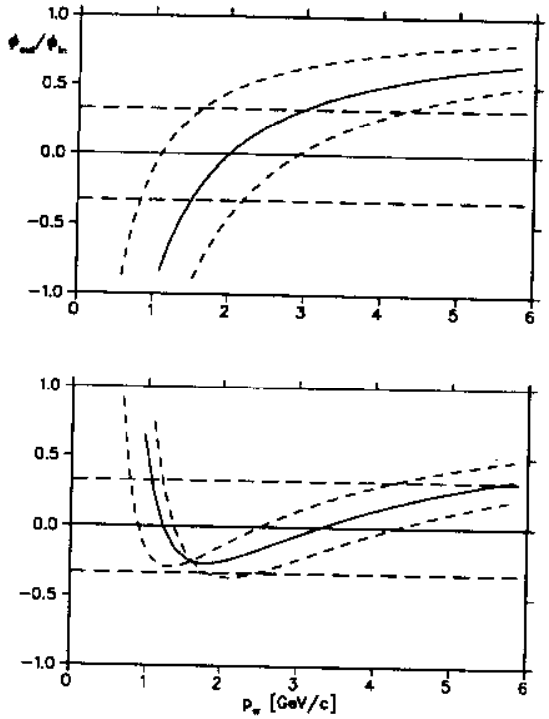

Figure 2: θ_{out}/θ_{in} vs momentum in thin lens focus systems, solid lines are for target center, dashed lines are from target ends; a) for single lens focussing; b) for two lens focussing.

Using this approach to match from the initial lithium lens of length ℓ_1, we place the second lens at a distance $2\,\ell_1$. The radius a_2 is set equal to that of the decay channel, and the length is

$$\ell_2 \approx \frac{a_2\, p}{3\,\ell_1\, B_2\, c} \tag{16}$$

which for a maximum field of $B_2 = 3.3\,T$ gives $\ell_2 = 15\,cm$ at 1 GeV/c, rising linearly with momentum.

2.2.4 Parameters of Systems

Using the above criteria we have designed lithium-lens and quadrupole channel systems for the mean captured momenta, corresponding to initial proton momenta of 10, 30 and 100 GeV/c.

Proton mom.	GeV/c	10	30	100
Nom. π mom.	GeV/c	1.3	2.4	5
First Li Lens				
Surface field	Tesla	10	10	10
Total length	cm	40	40	40
Nominal length	cm	31	31	31
Radius	cm	10	5	2.5
Space	cm	60	60	60
Second Li Lens				
Surface field	Tesla	3.3	3.3	5.7
Total length	cm	20	36	40
Radius	cm	15	15	15
Decay channel				
Pole tip fields	Tesla	6	6	6
Quad. length	cm	15	20	30
Gap length	cm	20	20	20
Decay length	m	400	800	1600

Table 2: Lithium and Quadrupole Channel Parameters

2.3 Solenoid Focussing

2.3.1 Capture from Target

If the capture is done inside a solenoid, then the calculations are very simple. The required maximum radius a_{sol} is

$$a_{sol} = 2 \frac{\hat{p}_t}{B_{sol}\, c} \tag{17}$$

where $\hat{p}_t$ is the is the maximum transverse momentum in units of eV/c. This radius is seen to be independent of momentum p. For the near ideal $\hat{p}_t = 0.6\ GeV/c$ and a conventional superconducting field $B_{sol} = 10\,\mathrm{T}$, the radius would be 40 cm which is very large and would correspond to a very large emittance. But hybrid solenoids can be made with fields as high as 45 Tesla (4). If we used a field of 33 T, then the radius with the same assumptions, would be only 7.5 cm. At lower momenta, a somewhat lower maximum $\hat{p}_t$ may be acceptable, for $a_{sol} = 7.5\ cm$, and $B_{sol} = 28\,\mathrm{T}$ the maximum transverse momentum captured is 0.31 GeV/c.

The solenoid length ℓ_{sol} to focus pions, at a fixed momentum p is

$$\ell_{sol} = \frac{\pi}{2}\,\beta = \pi \frac{p}{B_{sol}\, c} \tag{18}$$

which rises with momentum. For a 28 T field, the length is 37 cm for 1 GeV, rising to 150 cm for 4 GeV. But one notes that for a long solenoid, the beam will be captured in the solenoid at all momenta, and for all source positions, an almost ideal situation. In this case, the normalized acceptance of the resulting beam is

$$\mathcal{A}_n(\mathrm{sol}) = \frac{a_{sol}\hat{p}_t}{m_\pi} = \frac{2p_t^2}{B_{sol}cm_\pi} = \frac{a_{sol}^2 B_{sol} c}{2m_\pi} \tag{19}$$

In practice we cannot maintain such a solenoid over any significant length and must match it into a lower field decay channel.

2.3.2 Decay Channel

For a solenoid decay channel we chose a field of 7 Tesla, which is easily attainable with superconducting magnets. The value is a little higher than that taken for the quadrupole pole tip fields, since the fields seen by the conductors in a quadrupole will be somewhat higher. We take the radius of the channel to be the same as that in the quadrupole case, i.e. 15 cm.

The acceptance of this channel will be seen to be the same as that for the 7.5 cm, 28 Tesla capture solenoid. If a suitable wide band matching can be provided, then all pions captured by the target solenoid will be transferred to the channel, independent of their momentum.

2.3.3 Match

The match between the target capture solenoid and the decay channel solenoid can be made without significant loss if the field and radius are varied so as to maintain the same acceptance, and if the rate of change of β with z is small compared with one. Defining $d\beta/dz = \epsilon$, we obtain (5)

$$B = \frac{B_o}{1 + \alpha z} \tag{20}$$

$$a = a_o \sqrt{1 + \alpha z} \tag{21}$$

where

$$\alpha = \frac{cB_o\epsilon}{2p} \tag{22}$$

It is found that for values of ϵ less than 0.5 there is negligible loss of particles. Fig. 3 shows the field and dimension profiles of such a match.

2.3.4 Parameters of Solenoid Systems

In table 3, parameters are given of solenoid capture and channel systems optimized for pion momenta of 0.5, 0.9, 1.3, and 2.8 GeV/c; corresponding approximately to the peak pion production from proton momenta of 3, 10, 30 and

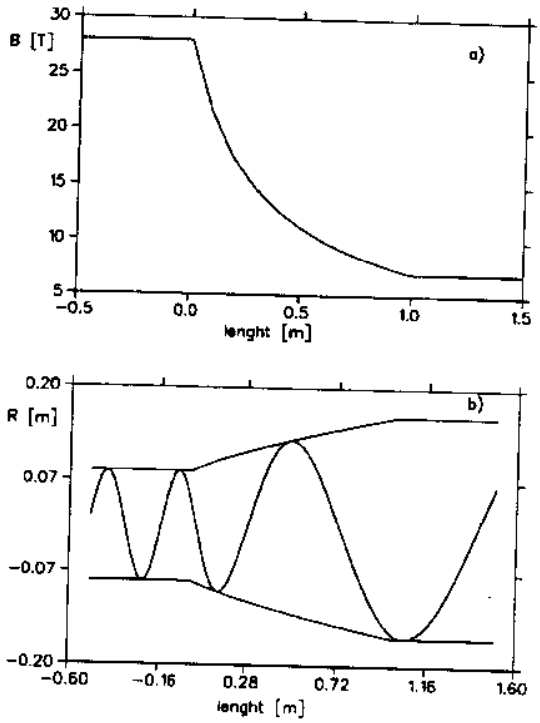

Figure 3: Solenoid Matching: a) Magnetic field vs. length; b) Radius vs. length, with a typical trajectory of a particle.

100 GeV/c. These pion momenta are lower than those given for the lithium lens-quadrupole case, see Table 2; reflecting the loss of low momenta particles from the channel cutoff in the lithium lens-quadrupole case.

Proton mom.	GeV/c	3	10	30	100
Nom. π mom.	GeV/c	0.5	0.9	1.3	2.8
Target length	cm	24	24	24	24
Capture field	Tesla	28	28	28	28
Solenoid radius	cm	7.5	7.5	7.5	7.5
Transition length	m	0.5	0.9	1.3	2.8
Channel field	Tesla	7	7	7	7
Channel radius	cm	15	15	15	15
Decay Length	m	100	200	340	500

Table 3: Solenoid Focus and Channel Parameters

3 MONTE CARLO RESULTS

3.1 Monte Carlo Program

A Monte Carlo program has been written to give a first approximation to the performance of the capture systems described above. The program, at this time, contains many approximations and the results obtained from it must be taken with some caution.

- Pion production spectra use the Wang (6) formulation. These distributions were derived by fitting proton proton interaction cross sections. The π multiplicities are slightly lower than those given by H Boggild and T. Ferbel (7) and significantly lower than those given by a nuclear calculation for Cu (8). Our estimates should thus be conservative.

- The pion momentum distributions given by the Wang formula are peaked somewhat lower than those given by the nuclear calculation for hydrogen, but higher than that given by the calculation for Cu. Clearly, the use of the Wang formula is unsatisfactory, but the qualitative results obtained are probably correct.

- Particles were followed using the paraxial approximation. This is a reasonable approximation for the production at 10 GeV and above, but is a poor approximation for pions produced by protons below 3 GeV.

- The program assumed that all particles are relativistic. This again is a poor approximation for proton production below 3 GeV.

- The initial proton beam was assumed to have an rms transverse radius of 1 mm, and a divergence of 1 mrad. The target was taken to be Cu with an interaction cross section of 0.782 barns. Pions passing through the target were reabsorbed with a cross section 2/3 of the above, and no tertiary pion production was included. Coulomb scattering, energy loss and straggling were calculated from Gaussian formulae. The pion decay lifetime was taken to be $2.603 \times 10^{-8}\,s$, the branching ratio into muons was assumed to be 100%. The kinetic energy distribution of decay muons was taken to be flat. Pions or muons which exceeded the aperture of focus components were assumed lost.

3.2 Results of Simulations

Table 4a gives the muon production for different initial proton energies, for the two capture systems described above: a) lithium lenses and quadrupole channel; b) solenoid capture and channel. The "capture % " given is the

fraction of pions that decay into muons that remain always within the focus channel. These fractions, particularly in the case of solenoid focussing, are relatively insensitive to the details of the pion production as given by the Wang formula. The "μ/p" ratio is the product of the "capture % " and the average charged pion multiplicity ("π mult."), and gives the final number of muons produced per initial proton. The average μ momentum is that found in the decay channel at the end, and the "rms mom. %" is the rms muon momentum spread divided by the average.

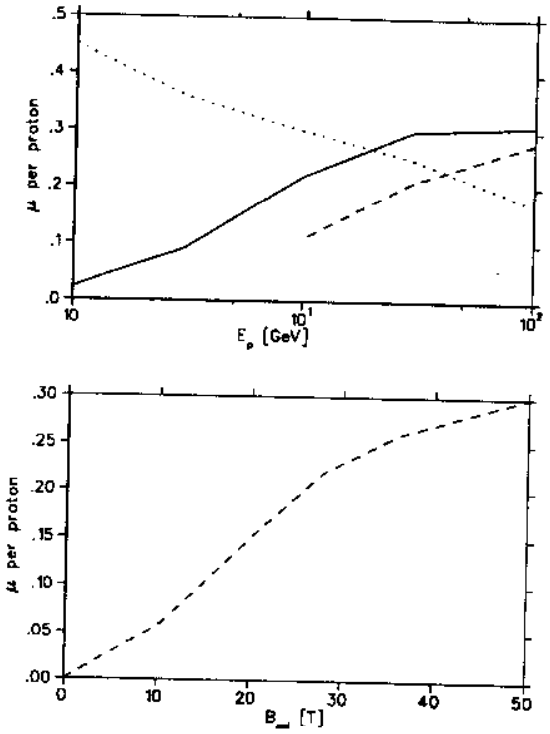

Figure 4: Monte Carlo Results: a)Muons per proton vs. proton energy; dashed line is for lithium lens system; solid line is for all solenoid systems; dotted line is capture efficiency for solenoid systems; b)Muons per proton vs. solenoid field.

Fig. 4a shows the calculated number of muons per proton for the different cases. It is seen that the lithium lens + quadrupole channel systems are universally worse than the solenoid systems; although the difference is shrinking as higher proton energies are used. In the all-solenoid cases the production increases with proton energy, but the increase levels off above 30 GeV. The dotted line in this figure shows the capture efficiency for the solenoid case. In reality this efficiency would be less at the lowest energies because of production in the backward direction that is not represented by the Wang formulation.

Table 4b and Fig. 4b show the dependence of muon production on the capture magnetic fields. All cases are for solenoid focussing from 10 GeV protons. As expected, the production rises monotonically with field, but the gain begins to saturate at fields above about 30 Tesla.

Table 4c compares capture efficiency (at 10 GeV with solenoid focussing) for a 60 cm long, 1 cm radius beryllium target with that from the shorter copper targets assumed above. It is seen that there is little difference between them. It must be noted however that this comparison does not include any differences in the production multiplicities or distributions.

Method	p Energy GeV	capture %	π mult.	μ/p	ave μ mom. GeV/c	rms mom. %
Li lens + quads	100	15	1.8	0.28	8	120
	30	17	1.2	0.21	2.3	70
	10	16	0.7	0.11	1.1	60
Solenoid	100	17	1.8	0.31	1.5	110
	30	25	1.2	0.30	1.0	140
	10	30	0.7	0.22	0.6	80
	3	35	0.3	0.09	0.34	60
	1	46	0.05	0.023	0.14	66

a) Dependence on proton Energy

Solenoid Field Tesla	Channel Field Tesla	capture %	μ/p	ave μ mom. GeV/c
20	5	22	0.15	0.46
28	7	30	0.22	0.60
36	9	37	0.26	0.61

b) Dependence on capture Magnetic Field

Tgt Material	Tgt length cm	Tgt rad. mm	capture %	μ/p	ave μ mom. GeV/c
Copper	24	3	31	0.22	0.6
Beryllium	60	10	29	0.20	0.6

c) Dependence on target materials

Table 4: Muon Production from Monte Carlo Studies

3.3 Choice of Proton Energy

Using a high field solenoid for capture, we find that the capture efficiency rises as the energy falls, at least down to a proton energy of 3 GeV. Similarly, the number of muons made per unit of beam energy also rises, at least down to an energy of the order of 3 GeV. Thus from the point of view of muon production economy and efficiency, it seems desirable to use this relatively low energy.

But as the proton energy falls, a larger number of protons are needed to obtain the required number of muons if we assume a single bunch targetting. Problems might arise from targeting larger bunches, and severe space charge problems arise in the proton ring used to bunch them prior to extraction and targeting. The tune shift in a ring whose mean bending field is B_{ave}, for a Gaussian bunch of length σ_z, is given by

$$\Delta\nu = \frac{N\, r_o\, m_p}{\sqrt{2\pi}\; 2\; \sigma_z\; \gamma_p\; \epsilon_n\; B_{ave}\; c} \tag{23}$$

where N is the number of protons in the bunch, r_o is the classical radius of the proton, m_p is the proton mass in electron volts, γ_p is the energy of the proton divided by its mass, ϵ_n is the rms normalized emittance of the protons and c is the velocity of light.

If longitudinal emittance of the muons is to be kept as low as possible then the proton bunch length must be less than a value, obtained from a Monte Carlo study of phase rotation, which is proportional to the average pion momentum,

$$\sigma_z \approx 3.0\,[m]\sqrt{\frac{1}{\gamma_p}} \tag{24}$$

For B_{ave} of 4 Tesla, an rms normalized emittance of 62 mm mrad (95 % emittance of 375 π mm mrad), and values of N such as to give 10^{13} muons using a 28 Tesla solenoid system, then we obtain the tune shifts given in Table 5 and Fig. 5. In this table and figure the proton beam power is also given.

Proton energy	GeV	3	10	30
Protons required	10^{13}	2 x 11	2 x 4.5	2 x 3.3
Proton beam power	MW	3.2	4.3	9.5
Bunch len. req.	m	1.7	1	0.58
Tune Shift		0.8	0.17	0.07

Table 5: Proton Source parameters

Assuming a largest acceptable tune shift of about 0.2 would indicate a preferred proton energy of 10 GeV. At this energy, the total required number of

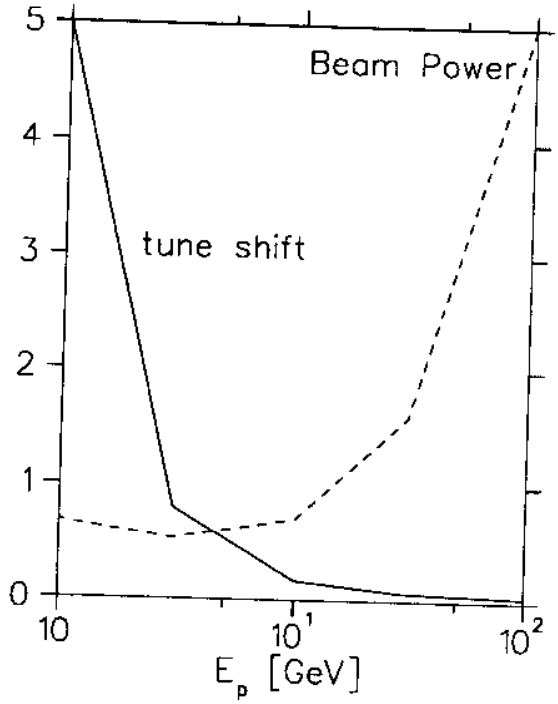

Figure 5: Choice of Proton Energy: the continuous line shows the tune shift, and the dashed line the relative proton beam power, each plotted vs. the proton beam energy.

protons (0.9×10^{14}), and the required repetition rate of 30 Hz are also close to the specification of the spallation source studied at ANL (9) and may thus be taken as reasonable values. It is noted however, that in such rapid cycling machines, the average bending fields are far less than the value of 4 T assumed above. Thus, in order to bunch without excessive space charge tune shift, we would require an additional fixed field superconducting bunching ring. This tune-shift limit is valid for a single bunch in a circular machine. The limit can be evaded in a linear machine or in schemes where multiple bunches are arranged to be targetted simultaneously, for example, by using dog-legs as "delay-lines", multiple rings or multiple synchronized kikers.

4 CONCLUSION

4.1 Caveats

It must be emphasized that the above calculations contain many approximations. In particular, pion production spectra used are those given by an approximate formula that was obtained by fitting proton-hydrogen data, rather

than proton-Cu as assumed in most cases here. The tracking program used the paraxial approximation and assumed that all particles were relativistic. These are poor approximations for proton production much below 3 GeV.

4.2 Solenoids vs. Lithium Lenses and Quadrupole Channels

Despite the approximations used in this study, it seems clear that the use of high field solenoids for both capture and decay channels is to be preferred over the use of lithium lenses and quadrupole channels.

- Given a capture solenoid approaching 30 Tesla, the absolute capture of muons per initial proton appears higher than with any plausible lithium lens system, at all energies. It is clearly superior for proton energies of 10 GeV and below.

- The use of a solenoid, instead of lithium lenses, allows the use of the same target, capture and decay channel for both signs of pions. This would be a significant saving. It may not, however, allow the use of muons of both signs from a single proton bunch. If rf is used to bunch rotate the muons, the polarity of this rf has to be different for the two signs.

- The technology of high field solenoids is more mature than that of large lithium lenses. Life time is less likely to be a problem, although questions of radiation damage must be studied.

4.3 Choice of Proton Energy

The proton beam energy required per muon, falls with proton energy down to a value around 3 GeV, but the number of protons required per bunch rises and the tune shift problems in the proton accelerator also rise as the energy falls. A reasonable compromise appears to be around 10 GeV.

4.4 Proposed parameters

On the basis of the above considerations, we propose the use of

- Solenoid capture, using a 28 Tesla 7.5 cm radius magnet.

- 10 GeV protons, using two bunches of $3 - 5 \times 10^{14}$ protons.

- We expect at least 0.2 muons per proton, thus generating $6 - 10 \times 10^{12}$ muons of each sign. This appears adequate to assure final bunches of 2×10^{12} in the collider, yielding, with the other parameters given in table 1, a luminosity of $10^{35}\ cm^{-2}\ s^{-1}$.

5 Acknowlegement

This research was supported by the U.S. Department of Energy under Contract No. DE-ACO2-76-CH00016 and DE-AC03-76SF00515.

6 REFERENCES

1. D. V. Neuffer, R. B. Palmer, Proc. European Particle Acc. Conf., London (1994)
2. R. J. Noble, *Advanced Accelerator Concepts*, AIP Conf. Proc. **279** (1993) 949
3. R. B. Palmer, *Magnetic fingers*, Proc. of the Informal Conference on Experimental Neutrino Physics, Cern 65-32 (1965), C. Franzinetti editor.
4. Physics Today, Dec (1994), p21-22
5. R. Chehab, J. Math. Phys. **5** (1978) 19.
6. C.L. Wang, Phys. Rev. **D10** (1974) 3876.
7. H. Boggild and T. Ferbel, Annual Rev. of Nuclear Science, 24 (1990) 74
8. D. Kahana, private communication.
9. Yang Cho, et. al., ANL-PUB-081622, *Proc. Int. Collab. on Advanced Neutron Sources*, Abbingdon, UK., May 24-28 (1993).